SEAMLESS AUTOMATIC MOSAICKING
TAKING INTO ACCOUNT INFRASTRUCTURES AND BUILDINGS

R. Xandri, F. Pérez, V. Palà, R. Arbiol

Remote Sensing Department, Institut Cartogràfic de Catalunya, 08038 Barcelona, Spain (rxandri, fernandop, vpala, rarbiol)@icc.es

Commission I, WG I/4

KEY WORDS: Earth Observation, Automation, DEM/DTM, Imagery, High Resolution, Multiple Images.

ABSTRACT:

When covering an extensive area by means of geocoded airborne or satellite imagery there is a need to combine a fairly large number of single images into a big, seamless mosaic. To accomplish this objective, all photo shots must be radiometrically compensated after geocoding to get a continuous, homogeneous result. Then, seam lines that define the contribution of each photo to the final mosaic are found. The final orthoimage can be evaluated in terms of geometric quality paying attention to several kinds of common artifacts. Two of them will be considered here: stretched areas and geometric shadows. Stretched areas -where ground sampling distance is worse than nominal due to observation geometry- can usually be avoided in the mosaic process. Geometric shadows, however, need a post-processing step on the final orthoimages in order to be properly eliminated. This automatic algorithm to obtain a high geometric quality mosaic is a key issue towards a generic procedure for true-ortho generation.

1. INTRODUCTION

Orthophoto projects usually consist of several hundreds of photo shots that must be combined to produce a radiometrically and geometrically continuous series of orthoimages. These orthoimages must maintain, at the same time, good radiometric properties regarding contrast and dynamic range (see Figure 1). A possible approach is to remove the physical radiometric effects in order to obtain homogeneous images that maximize the probability of obtaining good continuity. After the mosaic is complete, local contrast enhancement and color balancing techniques are used to obtain a high contrast orthoimage.
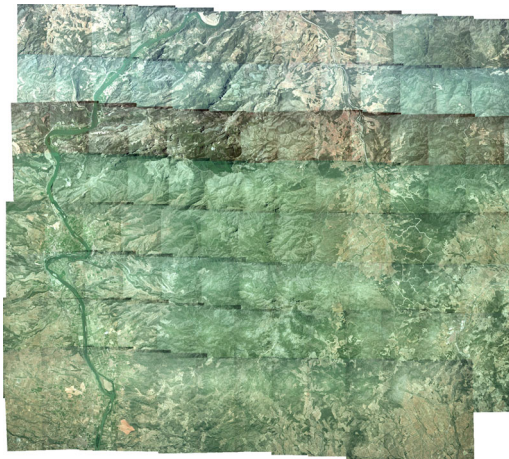

Figure 1. Block composed by 95 shots before radiometric corrections

Most mosaicking algorithms apply some kind of feathering-like techniques to join the different mosaic pieces (Knopp & Gerhard, 1998; Neusch & Grussenmeyer, 2002). They have been discarded for our purposes due to the blurring originated by numerous small geometrical disparities, especially when working in projects involving large scale photographs.

In our approach the first step is to eliminate -or, at least, reduce as much as possible- the radiometric differences between adjacent shots (see Figure 2). These differences are mainly due to temporal and spatial variations between acquisitions and also to artifacts introduced during the digitization process (Xandri et al., 2005b).

Figure 2. The same block, after radiometric balance

Once both overlapping images have been radiometrically brought together as much as possible, a seam path can be defined that separates the contributions from both images to the mosaic. These seams are found following the procedure described in (Xandri et al., 2005a). In this approach, a cost image is defined on the overlapping part between every pair of images (see Figure 3) and a set of departure and arrival pixels are marked out as origin and end of the seam. A path with a minimum cost is then found connecting the two aforementioned sets. A sensible definition of the cost function and the departure and arrival sets is the key point to obtain a good final mosaic avoiding non-desired artifacts.
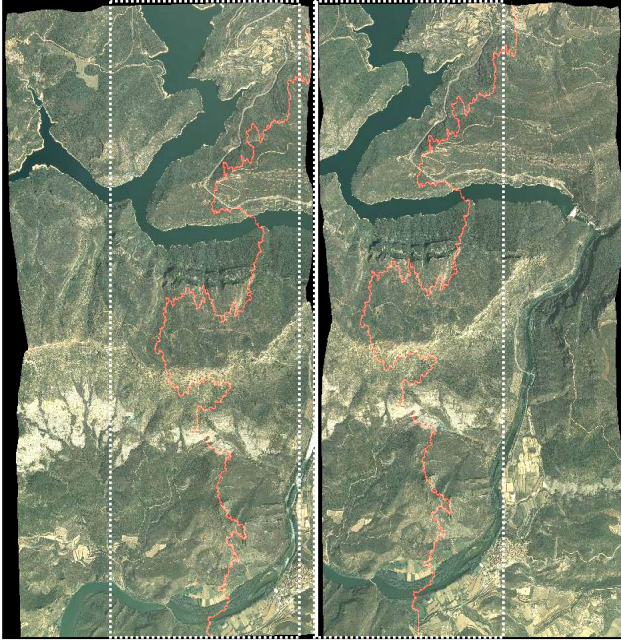
Figure 3. Pair of shots sharing a common area. The seam line that divides the contribution of each shot will be computed inside this area

This same method is applied to find a seam path for every pair of consecutive images in a large block. However, the problem of connecting the individual seams to generate the polygon that defines the image pixels contributing to the final mosaic is not trivial and is addressed at (Xandri et al., 2005b).

Two main artifacts can still be perceived in the resulting images that degrade the product quality: stretched areas and geometric shadows or occlusions (see Figure 4). In this paper we shall try to accurately describe these two effects and define a strategy to overcome the drawbacks they pose on the image.
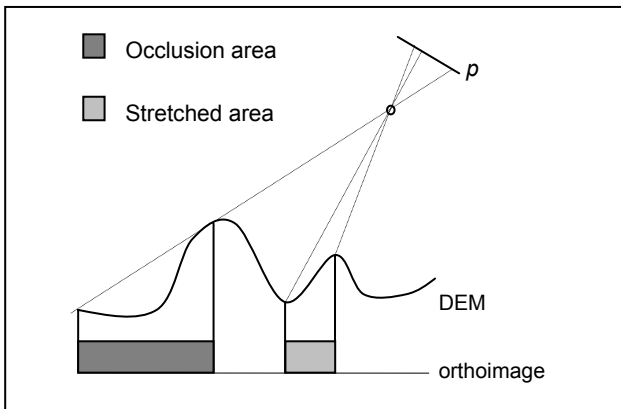

Figure 4. Geometric description of stretched and occlusion areas

2. STRECHED AREAS

2.1 Definition

To illustrate the concept of a stretched area, let's imagine we are observing a spherical object as shown in Figure 5.
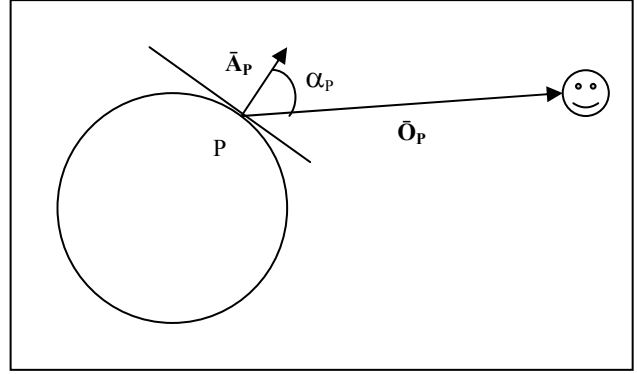

Figure 5. Image quality depends on the observation angle

Let $\bar{A}_P$ be the vector normal to the sphere in point P and $\bar{O}_P$ be the Observation vector from point P to the observer and let's define α_P as the angle between these two vectors. It is easy to see that we have the best view for areas with $\alpha_P = 0°$. Conversely, regions with $\alpha_P > 90°$ are not seen by the observer. We can now define the Stretch Factor S_P as:

$$S_P = \cos^2\left(\alpha_p\right) = \left(\frac{\left\langle \vec{A}_p, \vec{O}_p \right\rangle}{\left\|\vec{A}_p\right\| \cdot \left\|\vec{O}_p\right\|}\right)^2 \tag{1}$$

Thus, the closer is S_P to one, the better quality is assigned to this point in terms of stretching. Since our aim is that a pixel in image space is not projected into two different pixels in the resulting orthoimage, values of S_P below 0.5 should be avoided in the final mosaic (see Figure 6). So, a stretching map in ortho space must be created for every photo shot and the relevant information belonging to the overlapping parts must be incorporated to the cost function.
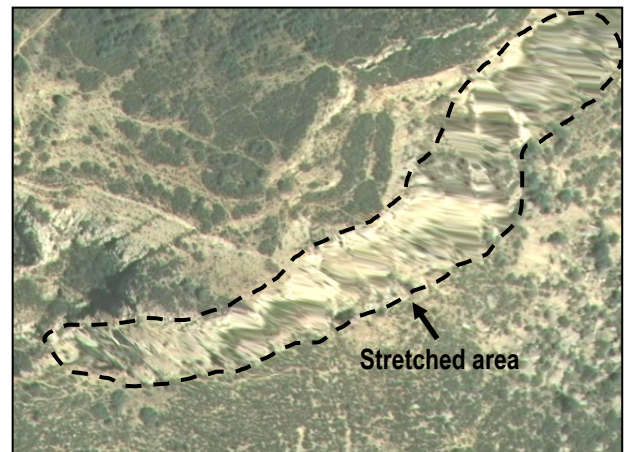

Figure 6. Detail of a stretched area. Poor quality pixels prevent the generation of a good orthophoto

2.2 Processing

In order to do so, a threshold is chosen for these stretching maps and they are binarized accordingly. From each of them, a set of blobs is extracted and added to an ordered list following certain criteria (size, stretching factor, position, etc.). This way, when

two stretched areas overlap the worse of them (in the sense of the chosen criteria) will be selected as the candidate to be eliminated. The remaining one still has the chance to be removed in subsequent mosaicking operations.

Starting from this list, a set containing the maximum allowable number of disjoint blobs is selected and two graphs are created, each one connecting the maximum number of blobs belonging to just one of the shots. If we appropriately connect each graph to the correct edge of the cost image and a high cost is assigned to all the pixels belonging to the graphs, we can guarantee that a seam path not attaining this value will necessarily separate these two graphs (see Figure 7).
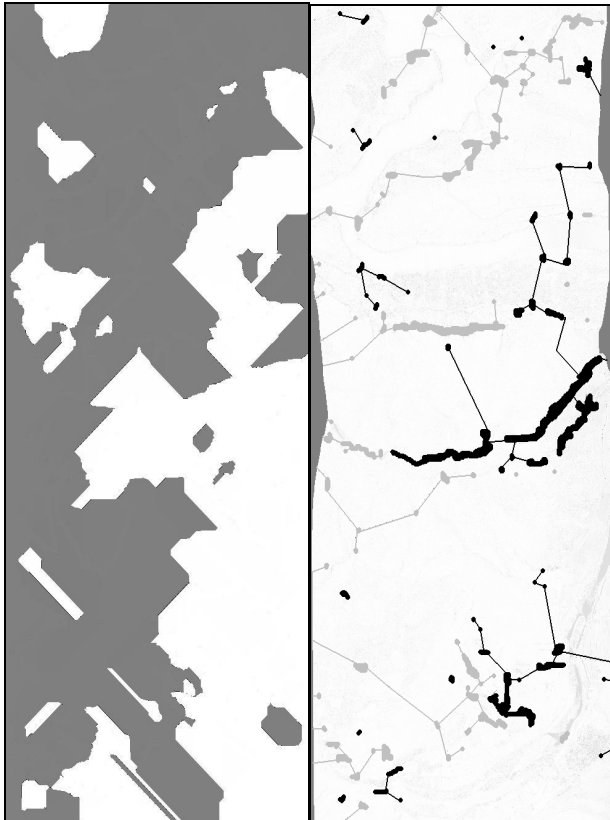

Figure 7. Stretching map of two shots sharing a common area. Graphs (right) are generated using the influence zones of the stretched areas (left)

Thus, a small modification on the general algorithm referenced in (Xandri et al., 2005b) plus a small fraction of extra computer time allows us to avoid most of the stretched areas during the normal mosaic procedure.

3. GEOMETRIC SHADOWS

3.1 Definition

An occlusion is intuitively easy to define. Figure 4 depicts in dark grey a ground area that cannot be seen by the observer because a feature on the terrain (not necessarily man-made) blocks the view. Depending on the kind of geocoding process we apply, the final geocoded image will present either a black blob (a hole) or a duplicated portion (ghosting effects) of the original image (Braun, 2002).

Since the occlusions can be calculated at geocoding time, it would be feasible, in principle, to take them into account in the standard mosaicking process. There are, however, two main reasons against. First, the inclusion of occluded areas in the cost image greatly increases the complexity of the seam and usually makes the final cost higher. In addition, it is often much simpler the processing of the final occlusions left in the orthoimage than the treatment of all geometric shadows for every pair of images.

Another good point in favour of a post-processing approach, as (Schickler & Thorpe, 1998) do, is that this very same procedure can be applied to correct the small defects sometimes found in the resulting map in the Quality Control (QC) step (local DEM changes, updates, etc.)
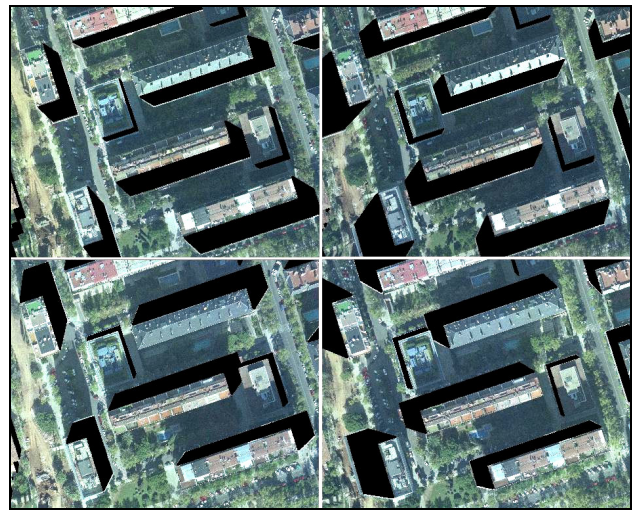

Figure 8. Occlusion maps of four shots. These acquisitions are enough to solve all the mosaic occlusions

The point is then the generation of occlusion maps in ortho space that consists of the following steps:

1. For every point in the orthoimage and every shot that contributes to the mosaic, the distance between this point and the observation position is calculated and associated to the corresponding pixel in the shot space.

2. If the position for this pixel has been already used, the annotated distance must be checked. If the calculated distance is shorter than the annotated one, it is substituted and the former pixel is marked as an occlusion. Otherwise, the actual pixel is marked.

In the end, an occlusion map in ortho space for every photo shot will have been created. An example of occlusion maps corresponding to four different shots can be seen in Figure 8.

3.2 Processing

Now we have the preliminary mosaic, the occlusion maps and the seam paths defining the contribution of each shot to the final image. Next task to be done is the combination of all occlusion maps into a single map of holes to be filled in the so called preliminary mosaic. Figure 9 depicts the result of combining the four occlusion maps shown in Figure 8.

Figure 9. Detail of the occlusion areas that remain at the end of mosaicking process

For each of these remaining geometric shadow areas, an analysis is performed in order to fill the gap with the smallest number of contributions from other photos. In Figure 10, different grey levels represent different combinations of shots that can be used to fill the gaps in the preliminary mosaic. This information must be analyzed to decide which shot solves each occlusion. The rule we have chosen is to sequentially select, from the whole list, the photo that covers the largest part of the remaining hole. Once all gaps have been processed we obtain, for every contributing image, a list of patches to be added to the mosaic.
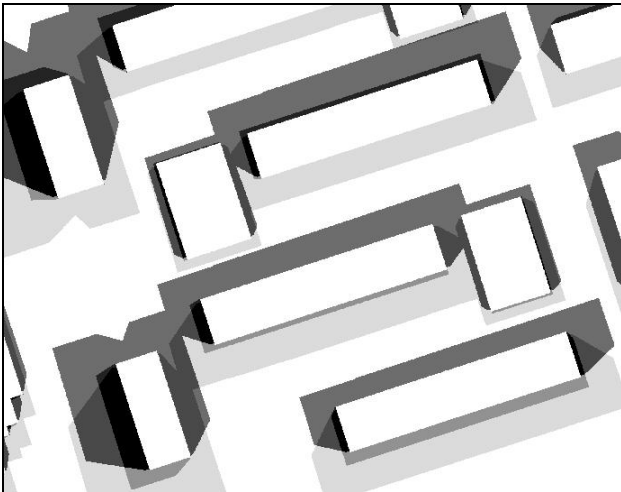

Figure 10. Occlusion intersections from four shots.

Each patch map must then be combined with the corresponding occlusion map to calculate the seams that allow the filling of the mosaic gaps without addition of new ones.

3.3 Shot contribution

First of all, a cost image is generated through the evaluation of the radiometric differences between the geocoded shot and the preliminary mosaic (Xandri et al., 2005a). Obviously, some zero cost areas will appear where this shot has already contributed to the mosaic.

Then, a simple graph is created from the occlusion map for this shot, overlapped on the difference image and connected to a random point on its edge. All pixels belonging to the graph are marked with a high cost value.

At last, the pixels corresponding to the patch map are also given a high cost and added to the cost image. Then, each of the patches is connected to the occlusion graph by means of a high cost line.

The objective is now to generate a set of closed seams encircling every patch to be added to the mosaic. With this purpose, we must select a departure point adjacent to the segment connecting the patch to the graph and an arrival point just at the other side of the segment (see Figure 11). With all these constraints posed, the general seam algorithm is applied on every patch and a minimum cost seam path is found guaranteeing that no new occlusions are added to the final mosaic.
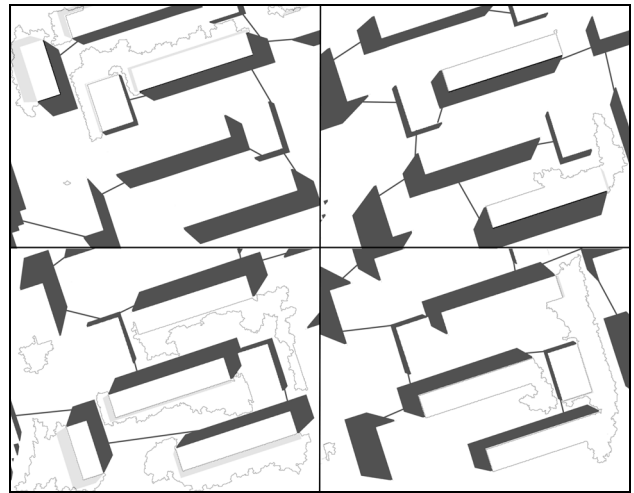

Figure 11. Pieces that solve the occlusions using different shots

After the processing of all the photographs in the list, the occlusion areas have been removed taking into account the contributions from other photos by means of small seamless mosaics. The final mosaic for these shots is shown in Figure 12.
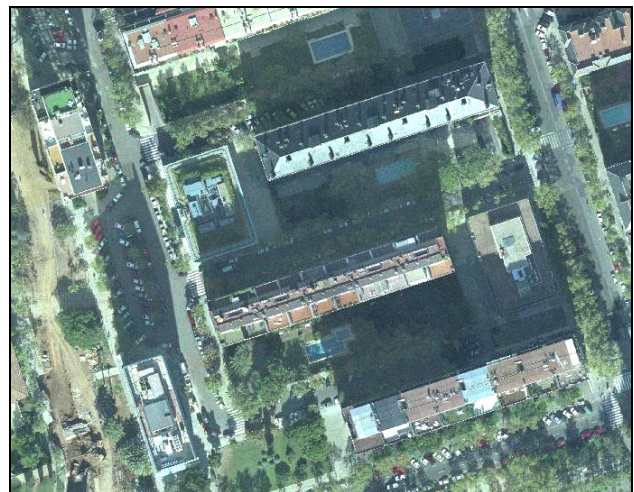

Figure 12. Final result of the whole process

As already stated, the first step consists in the detection of occlusion areas. Therefore, it is necessary that the DEM used for image rectification accurately represent the element that generates the occlusion. Nevertheless, our experience shows that these inaccuracies are not critical.

For example, if we have uncertainties on the height of a given building, its rectification and the calculation of the geometric shadows will not be totally correct. Figure 13 shows that some areas of the building have not been displaced to their correct planimetric position, lying on the incorrect side of the occlusion. However, as the same areas will be located on other wrong positions for different acquisitions, high values will be generated on the difference images. Moreover, these areas of high differences are attached to the occluded zones. Our tests have shown that these areas are naturally eliminated when filling the occlusion area.
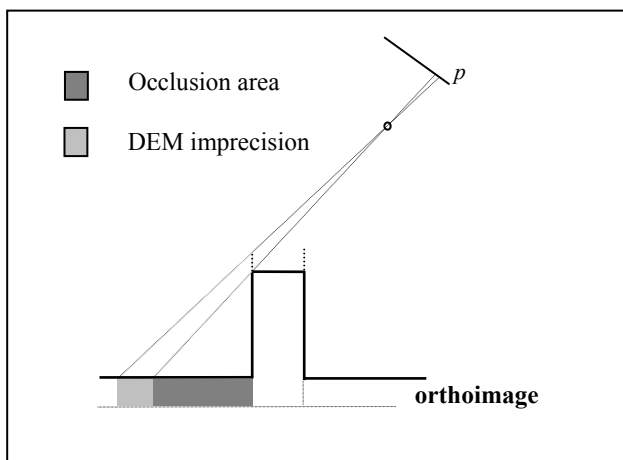

Figure 13. Anomalies caused by DEM inaccuracies

4. RESULTS

ICC started applying this automated mosaicking technique at the end of 2004 in the frame of a Project for the generation of 1:5000 orthophotos of Catalonia (a 32.000 Km² region located on the northeast part of the Iberian Peninsula) and the following biannual updates (Xandri et al., 2005b). The DEM used to geocode the images acquired in this project does not contain features over the ground and thus occlusions are not calculated or taken into account. However, this area includes a portion of the Pyrenees mountain range and therefore the stretching areas are frequent. Although it is difficult to quantitatively evaluate the improvements obtained, this new approach has proven good enough as to avoid any ulterior correction of stretched areas in the QC step of our processing chain.

The additional step for occlusion removal has been applied to two different projects. The first one focuses on the generation of a 1:2000 orthophoto series covering the city of Barcelona and its metropolitan area for the Catalonian Autonomous Government (Generalitat de Catalunya). This project was flown at a height of 2200 meters on 2005, generating 900 photos over an extension of 430 Km² with 60% overlapping on both directions using a DMC from Zeiss-Intergraph. The project was geocoded using a DEM that included road infrastructures but no buildings. Consequently, the occlusions of buildings were not addressed in this project. Figure 14 shows in detail the resulting mosaic after occlusion removal. The upper image contains occluded areas where the original image pixels have been duplicated (note some cars in the highway). The lower one presents the automated final mosaic where these artefacts have been eliminated.

Figure 14. Removal of occlusions due to infrastructures

In the second project, a color true orthoimage corresponding to an area of 1 Km² from Barcelona has been produced from aerial photography. The camera was a ZEISS RMK-TOP, mounting a 150 mm. focal length lens. The flight altitude was 750 m over the ground, corresponding to 1:5000 scale pictures. The final orthoimage pixel size is 10 cm and contains some multi-storey buildings along Diagonal Avenue. In order to fill the occlusions, a set of 22 photographs was taken with 80% overlapping in both directions (see Figure 15).

A Triangulated Irregular Network (TIN) obtained from the existing urban 1:5000 topographic map was created for the precise orthorectification of the photographs, having approximately 11000 points and 21000 triangles. The topographic map specifications are not ideal for true orthoimage generation, but one of the goals of the experiment was the determination and evaluation of the problems encountered when using this kind information (Palà & Arbiol, 2002).

The quality of the final product obtained using the presented technique, i.e. the number of occlusion zones that are not solved and the number of visible transition lines between images, depends on the radiometric similarity and the flight plan, see (Zhou et al., 2005). Figure 16 shows a detail of the final mosaic obtained.
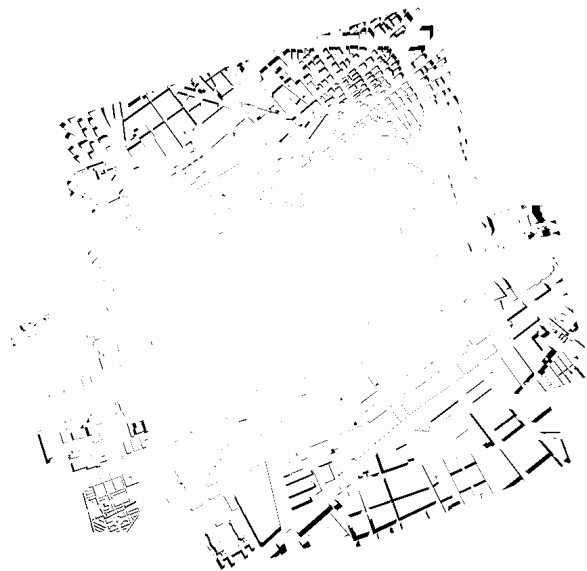
Figure 16. Final True-Ortho mosaic over Barcelona

Figure 15. Using a correct overlapping, all the occlusion areas from the center part of the image are removed (upper: before, lower: after)

5. REFERENCES

Braun, J., 2003. Aspects on True-Orthophoto Production. Proceedings, 49th Photogrammetric Week, pp. 205-214. Stuttgart, Germany.

Knopp, D., Gerhard, J., 1998. "Automating Image Mosaic Production". Earth Observation Magazine Vol. 7, Part 2. http://www.eomonline.com/Common/Archives/1998feb/98feb_knopp.html (accessed April 21, 2005).

Neusch, T, Grussenmeyer, P, 2002. Urban Imagery Combining Photogrammetric and Remote Sensing Techniques. Proceedings of the ISPRS Commision VI Symposium 2002, Vol. XXXIV, Part 6, ISSN 1682-1750.

Palà, V., Arbiol, R., 2002. True orthoimage generation in urban areas. Proceedings of 3rd International Symposium Remote Sensing of Urban Areas, Vol. 1, pp. 309-314. Istanbul, Turkey.

Schickler, W., Thorpe, A., 1998. Operational procedure for automatic true orthophoto generation. International Archives of Photogrammetry & Remote Sensing, Vol. 32, Part 4, pp. 527-532.

Xandri, R., Palà, V., Arbiol, R., 2005a. Determinación automática de costuras para la generación de ortofotos. Proceedings of 6th Geomatic Week. Barcelona.

Xandri, R., Pérez, F., Palà, V., Arbiol, R., 2005b. Automatic Generation of Seamless Mosaics over Extensive Areas from High Resolution Imagery. World Multi-Conference on Systemics, Cybernetics and Informatics (WMSCI). Orlando, USA.

Zhou, G., Chen, W., Kelmelis, J., Zhang, D., 2005. A Comprehensive Study on Urban True Orthorectification. IEEE Transactions on Geoscience and Remote Sensing, Vol. 43, Part 9, pp. 2138-2147.